LA-UR-81-3153

TITLE: PARTICLE TRANSPORT IN FIELD-REVERSED CONFIGURATIONS

AUTHOR(S): M. Tuszewski, R. K. Linford, J. Lipson, and A. G. Sgro



SUBMITTED TO: 4th Compact Toroid Symposium to be held at Livermore, California, October 27-29, 1981.



University of California

LOS ALAMOS SCIENTIFIC LABORATORY
Post Office Box 1663 Los Alamos, New Mexico 87545
An Affirmative Action/Equal Opportunity Employer

Form No. 836 R3
St. No. 2629

# Particle Transport in Field-Reversed Configurations

M. Tuszewski, R. K. Linford, J. Lipson and A. G. Sgro

## 1. Introduction

A field reversed configuration (FRC) is a compact toroid that contains no toroidal field. These plasmas are observed to be grossly stable[1] for about 10-100 μsec. The lifetimes appear limited by an n = 2 rotational instability which may be caused by particle loss.[2] Particle transport is therefore an important issue for these configurations. We investigate particle loss with a steady-state, 1-D model which approximates the experimental observation[1] of elongated FRC equilibrium with about constant separatrix radius.

## 2. Steady-state particle transport model

We consider an FRC with a 2-D (r,z) elongated equilibrium confined inside a straight cylindrical conducting wall. The balance between plasma and magnetic field pressures in this geometry imposes[1]

$$\langle \beta \rangle = 1 - \frac{1}{2} x_s^2 \quad , \tag{1}$$

where $\langle \beta \rangle$ is the average $\beta = P/(B_o^2/2\mu_o)$ over the separatrix volume. $B_o$ is the external magnetic field and $x_s$ is the ratio of separatrix to conducting wall radius. The constraint of Eq. (1) applies to any axial (z) position on the elongated portion of the FRC. We neglect end effects and consider a 1-D model where 2-D effects are included by using Eq. (1) as a condition on the radial profile. We assume a steady state where particle loss across the separatrix is balanced by a source of particles from axial contraction. We assume uniform temperatures $T_e$ and $T_i$, as suggested by the experimental data.[1] We further assume complete MHD stability and neglect self-consistent radial electric fields as well as flux annihilation at the field null. The steady-state radial diffusion equation is given by

$$\frac{1}{r}\frac{d}{dr}(r\Gamma) = \begin{cases} + n/\tau_c & r < r_s \\ - n/\tau & r > r_s \end{cases} \quad , \tag{2}$$

where $\tau_c$ is the time constant of the axial contraction and $\tau$ is the particle confinement time on open field lines. We take $\tau_c = \ell/2v_s$, where $v_s$ is the sound speed and $\ell$ is the length of the FRC to model present experiments where particles steadily flow along open field lines, without any end-plugging. We assume, from experimental observation,[1] that $\ell$ is about 70% of the coil length. In addition to Eq. (1), the second constraint on the radial profile comes from matching at the separatrix the particle fluxes from the closed and open field line regions. To satisfy this boundary condition, it is useful to introduce an auxiliary variable w with

$$[d\beta/dr]_{r_s} = -\beta_s/w_{i0} \quad , \tag{3}$$

where $\beta_s$ is the plasma $\beta$ on the separatrix. The quantity w is just the ratio of the gradient length at the separatrix to the vacuum ion gyroradius $\rho_{i0}$. The condition $r\Gamma(r_s-) = r\Gamma(r_s+)$ determines the value of w. The particle confinement time $\tau$ is defined as $N/2\pi r_s \Gamma_s$, where N is the number of particles per unit axial length within the separatrix and $2\pi r_s \Gamma_s$ is the radial flux of particles at the separatrix, per second and per unit axial length.

We take $r\Gamma = (r\Gamma)_C + (r\Gamma)_{LHD}$ where $(r\Gamma)_C$ is the classical (Spitzer) particle flux and $(r\Gamma)_{LHD}$ corresponds to anomalous transport from the Lower Hybrid Drift (LHD) instability saturated by wave energy bound.[1] A

quantitatively similar saturation level is obtained from electron resonance broadening.[4] Other saturation mechanisms such as ion trapping[5] yield higher saturation levels for the cases of interest in this work. It is found that typical FRC radial profiles have a classical core near the field null (r = R) and an anomalous region in the vicinity of the separatrix. The particle confinement times $\tau$, determined by LHD transport, will be shown to be in good agreement with the experimental data.[1] On the other hand, classical transport yields lifetimes which do not fit the experimental data. Integrating Eq. (2) from r = o to r = $r_s$, and using Eq. (3), one obtains

$$\tau = 4 \frac{(m_i/\pi m_e)^{1/2}}{(1 + T_e/T_i)\omega_{cio}} \cdot \frac{(1 - \beta_s)^{3/2}\langle\beta\rangle}{\beta_s} \cdot S \cdot w^3 \quad , \tag{4}$$

where $S = R/\rho_{io}$. Integrating Eq. (2) from $r = r_s$ to $r = r_w$, assuming an exponential tail for the pressure profile on open field lines, using Eq. (4) and particle flux continuity at the separatrix, one obtains

$$w^4 = (\ell S/8\, r_s) \cdot (\pi m_e/m_i)^{1/2} \cdot (1 + T_e/T_i)^{1/2} / (1 - \beta_s)^{3/2} \quad . \tag{5}$$

For given $m_e/m_i$, $T_e$, $T_i$, $B_o$, $r_w$, $\ell$, $x_s$, and for a given choice of w, Eq. (2) is integrated numerically for $r < r_s$, with the constraints of Eqs. (1) and (3). This determines the value of $\beta_s$, which in turn determines w with Eq. (5). By iterative procedure, the self-consistent values of w and $\beta_s$ are found and the confinement time $\tau$ is obtained from Eq. (4). The details of this calculation are contained in Reference 6.

## 3. Confinement times for FRX-B and FRX-C parameters

We consider recent experimental data of the FRX-B device,[7] and the FRX-C parameters as projected from a scaling code.[8] Those parameters and the theoretical values of $\tau$, $\beta_s$ and w are given in Table I for each case. The values of $\tau$ are also plotted in Fig. 1 as function of the variable $R^2/\rho_{io}$. We observe from Fig. 1 that the theoretical values of $\tau$ for the FRX-B device are comparable to the experimental values of the stable periods which are also indicated in Fig. 1. This is consistent with the theoretical picture of plasma spin-up linked to particle transport.[7] The empirical scaling $\tau(\mu sec) \sim 0.6\, R^2/\rho_{io}$ derived from the FRX-B results[4] is also indicated on Fig. 1. The theoretical points are in good agreement with this scaling, perhaps suggesting a somewhat stronger scaling $\tau \sim 0.8\, R^2/\rho_{io}$. Within the uncertainties of the experimental data and of the transport theory, there is good agreement between experiment, the LHD theory in this paper, and the numerical results of Hamasaki,[9] who first suggested the $R^2/\rho_{io}$ scaling. We observe from Fig. 1 that this scaling appears to approximately fit the projected performance of the FRX-C device. One should also note that this scaling only applies for deuterium ions. For other ion species, Eq. (4) shows a scaling of $\tau$ as $m_i$ rather than the $m_i^{-1/2}$ dependence suggested by the $R^2/\rho_{io}$ scaling.

## 4. Scaling of the LHD transport

We investigate the scaling of $\tau$ with the three parameters, S, $x_s$, and w, that control the radial $\beta$ profiles. These parameters usually vary simultaneously, but in order to test the sensitivity of $\tau$ to each of them, we vary only one parameter on a given scaling, keeping the other two constant.

The scaling with S corresponds approximately to the cases of Table I and Fig. 1 since, for these data, the variations of $x_s$, w, and $B_o$ are small. The numerical results suggest $\tau \sim R^2/\rho_{io}$, which is the empirical scaling discussed

in the previous section. In addition to this observed $R^2/\rho_{i0}$ scaling, the model predicts increased confinement time with increases in the values of $x_s$ and w.

It may be desirable to form FRC's with values of $x_s$ closer to unity in order to minimize pressure gradients as suggested by Eq. (1). We consider the FRX-C cases of Table I and vary $x_s$ from 0.45 to 0.8, while keeping $r_w$, S, w, $T_e$, and $T_i$ constant. The results of this scaling, given in Fig. 2, yield the approximate scaling $\tau \sim x_s^{3.3}$, so that an increase in $\tau$ up to a factor of seven may be obtained.

It is conceivable to improve the open field line confinement $\tau_\parallel$ by some end-plugging technique or by plasma injection. A corresponding increase in w may be obtained. We vary w for the FRX-C cases of Table I, at constant S and $x_s$. The results, given in Fig. 3, suggest $\tau \sim w^{1.6}$ and an increase of w from 1 to 3 yields about a factor of 6 increase in $\tau$. Furthermore, increasing w decreases the value of the drift parameter $v_d/v_i$ at the separatrix. This may greatly reduce anomalous transport if a different saturation mechanism such as ion trapping[5] is relevant in the weak drift parameter regime.

5. Comparison of various boundary conditions at the separatrix.

It has been shown above that the determination of the radial profile at the separatrix is crucial to the FRC confinement scaling. The detailed physics of this profile may involve two-fluid, electric field, electron temperature gradient and finite-orbit effects. In particular, it is of interest to evaluate the contribution to the pressure on open field lines of guiding centers inside the separatrix which are assumed not to suffer end loss. A 1-D transport code[9] is being used to compare various loss rates on open field lines that estimate this guiding center contribution. First, $\partial n/\partial t = n/\tau_\parallel$ is used, where $\tau_\parallel = \ell/2v_s$. This corresponds to the free streaming model of this paper. Second, an ad hoc reduction in loss rate is used with $\partial n/\partial t = (n/\tau_\parallel) \cdot \{1 - \exp[-(r - r_s)^2/\rho_{i0}^2]\}$. Third, the contribution of guiding centers inside the separatrix is calculated, and the loss rate on open field lines is decreased accordingly. This work is in progress.

References


1. W. T. Armstrong, R. E. Linford, J. Lipson, D. A. Platts, and E. G. Sherwood, Phys. Fluids (to be published).
2. D. C. Barnes and C. E. Seyler, in Proceedings of the US-Japan Joint Symposium on Compact Toruses and Energetic Particle Injection, Princeton, (1979), p. 110.
3. R. C. Davidson and N. A. Krall, Nucl. Fusion 17, 1313 (1977).
4. S. P. Gary, Phys. Fluids 23, 1193 (1980).
5. H. V. Fahrbach, W. Köppendörfer, M. Munich, J. Neuhauser, E. Röhr, G. Schramm, J. Sommer, and E. Holzhauer, Nucl. Fusion 21, 257 (1981).
6. M. Tuszewski and R. K. Linford, "Particle Transport in Field Reversed Configurations," Los Alamos National Laboratory report LA-UR-81-2319 (1981) (submitted to Phys. Fluids).
7. J. Lipson, W. T. Armstrong, J. C. Cochrane, K. F. McKenna, E. G. Sherwood, and M. Tuszewski, Appl. Phys. Lett. 38 680 (1981).
8. R. E. Siemon and R. R. Bartsch, Third Symposium on Physics and Technology of Compact Toroids in the Magnetic Fusion Energy Program, Los Alamos 1980, Los Alamos National Laboratory report LA-8700-C (1981), p. 172.
9. S. Hamasaki and N. A. Krall, Conference Record IEEE International Conference on Plasma Science, Montreal (1979) 5E10.

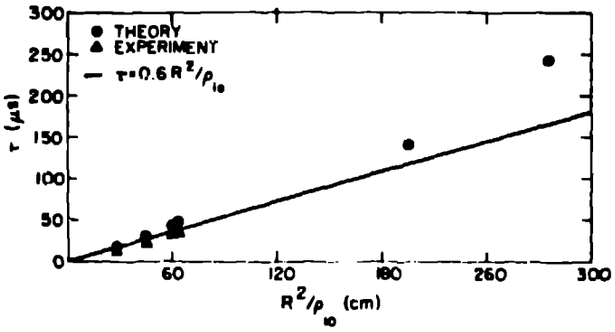


Figure 1
Scaling of $\tau$ with $R^2/\rho_{i0}$ for the FRX-B and C devices.

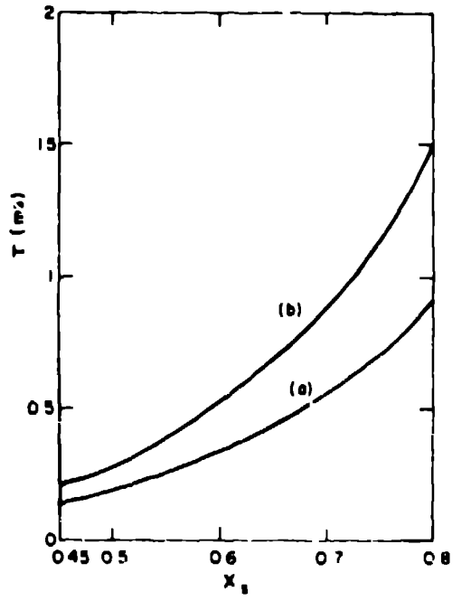


Figure 2
Scaling of $\tau$ with $x_s$
(a) FRX-C, S = 27
(b) FRX-C, S = 36

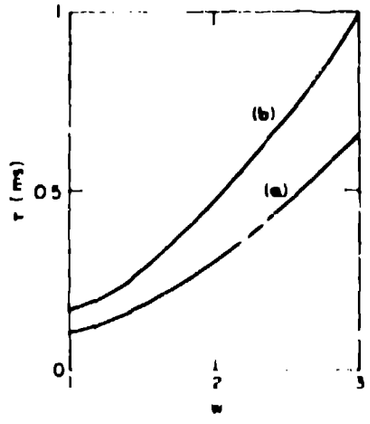


Figure 3
Scaling of $\tau$ with w
(a) FRX-C, S = 27
(b) FRX-C, S = 36

TABLE I
EXPERIMENTAL AND NUMERICAL FRC DATA

| Device | $P_0$ (mTorr) | $x_s$ | S | $T_i$ (eV) | $T_e$ (eV) | $n_e$ | w | $\tau$ ($\mu$s) |
|---|---|---|---|---|---|---|---|---|
| FRX-B | 9 | .44 | 7.1 | 870 | 150 | .56 | 1.1 | 1 |
| ($r_w$ = 12.5 cm) | 17 | .42 | 12.2 | 430 | 150 | .45 | 1.19 | 25 |
| | 29 | .47 | 14.5 | 190 | 150 | .40 | 1.17 | 4 |
| | 41 | .45 | 16 | 250 | 150 | .40 | 1.21 | 65 |
| FRX-C | 20 | .45 | 27 | 500 | 150 | .32 | 1.23 | 11 |
| ($r_w$ = 22.5 cm) | 40 | .48 | 36 | 250 | 150 | .28 | 1.31 | 240 |